

Deep Contrastive Multi-view Clustering under Semantic Feature Guidance

Siwen Liu¹, Jinyan Liu¹, Hanning Yuan¹, Qi Li¹, Jing Geng¹, Ziqiang Yuan¹,
and Huaxu Han¹

Beijing Institute of technology, China

Abstract. Contrastive learning has achieved promising performance in the field of multi-view clustering recently. However, the positive and negative sample construction mechanisms ignoring semantic consistency lead to false negative pairs, limiting the performance of existing algorithms from further improvement. To solve this problem, we propose a multi-view clustering framework named Deep Contrastive Multi-view Clustering under Semantic feature guidance (DCMCS) to alleviate the influence of false negative pairs. Specifically, view-specific features are firstly extracted from raw features and fused to obtain fusion view features according to view importance. To mitigate the interference of view-private information, specific view and fusion view semantic features are learned by cluster-level contrastive learning and concatenated to measure the semantic similarity of instances. By minimizing instance-level contrastive loss weighted by semantic similarity, DCMCS adaptively weakens contrastive learning between false negative pairs. Experimental results on several public datasets demonstrate the proposed framework outperforms the state-of-the-art methods.

Keywords: Multi-view clustering · Contrastive learning · False negative pairs · Semantic feature

1 Introduction

Multi-view clustering(MVC) has gained interest in the last few years and has been widely applied in the field of biology [48], medicine [7, 44], social network [47], agriculture [32], and so forth. Traditional methods for MVC include non-negative matrix factorization [46, 52], latent representation learning [17, 39], graph learning [18, 37], and tensor learning [2, 29]. Many of the traditional MVC methods suffer from poor representation and high computational complexity, resulting in limited performance in complex scenarios with real data [12]. Deep learning develops superior features with its strong representation ability, so deep MVC is becoming popular. Deep MVC methods can be categorized into four sub-groups: subspace clustering [22, 31], graph-based deep clustering [33, 38], deep representation clustering [34, 45], and spectral clustering [3, 27]. Compared to other approaches, deep representation clustering often employs a simple encoder-decoder structure and may be more flexible [10].

Effective deep MVC depends on learning discriminative common information from multi-view data. Recently, contrastive learning has been integrated into deep MVC because of its ability to capture high-level semantics while discarding irrelevant information [40]. Ke *et al.* [19, 20] design a fusion network to extract common information. Xu *et al.* [41] carry out distinct goals at different feature levels to resolve the conflict between consistency and reconstruction objectives. Hu *et al.* [15] establish triple features through contrastive learning using feature-oriented alignment, commonality-oriented, and cluster-level consistency. Even though these contrastive learning-based deep MVC methods have achieved important progress, there are still some issues that need to be resolved: (1) For directly applying contrastive loss such as InfoNCE [6], the performance of many methods (*e.g.* [15, 41]) is impaired by false negative pairs. Minimizing the contrastive loss may increase the feature dissimilarity of instances sharing the same cluster label due to false negative pairs, which contradicts with clustering objective and leads to unfriendly representation learning for clustering. (2) Some methods (*e.g.* [19, 20]) fuse specific views to obtain a fusion view containing common information. However, the view-private information is inevitably introduced to fusion view features and transferred to contrastive learning interfering with the quality of clustering.

In this paper, we propose a novel semantics-guided multi-view contrastive clustering framework to address the above issues. Our framework, as illustrated in Fig. 1, consists of a view-specific feature fusion module and a cross-view double-level contrastive module. In the view-specific feature fusion module, auto-encoders are used to generate view-specific features, and weighted fusion is employed to generate the fusion view features. The cross-view double-level contrastive fusion module employs two consistency objectives: semantics-guided instance-level contrastive learning and cluster-level contrastive learning. Instance pair weights measured by semantic features are applied to mitigate the impact of false negative pairs. Furthermore, in order to reduce the influence of view-private information, common information are concentrated when calculating instance pair weights. Compared with previous work, our contributions are as follows:

- A DCMCS framework is proposed to lessen the impact of false negative pairs in instance-level contrastive learning. The objective of contrastive learning is made consistent with the clustering objective by using instance pair weights obtained from semantic features to learn cluster-friendly features.
- When calculating the instance pair weights, the common information of the fusion view are concentrated in DCMCS. It relieves the interference of the view-private information in the fusion view to achieve better clustering results.
- In the experiment, we show how effectively the instance pair weights and the fusion view’s common information work. Experimental results on several public datasets demonstrate our framework outperforms the state-of-the-art methods.

The rest of the paper is organized as follows. The relevant work is presented in Sec. 2. The proposed framework is presented in Sec. 3. Comprehensive exper-

iments and findings are reported in Sec. 4. Sec. 5 provides the conclusion and future work.

2 Related Work

2.1 Multi-view clustering.

With the development of deep learning, deep MVC has an important position in MVC methods. The four categories of deep MVC methods are deep representation learning [8, 26, 34, 45], deep graph learning [23, 33, 38], subspace clustering [22, 30, 31], and spectral clustering [3, 27, 49]; the latter three are frequently combined [9, 24, 43]. In deep representation learning, contrastive methods [15, 34, 41], collaborative methods [45, 51], adversarial methods [26, 50], and distillation methods [8, 28] can be used to acquire common information. Yang *et al.* [45] optimize view features using intra-view collaborative learning and gain complementing information through inter-view collaborative learning. Li *et al.* [26] employ adversarial learning to further capture data distribution. A distillation approach is presented by Chen *et al.* [8] that uses a teacher model with complete views to direct a student model with lacking views. Contrastive learning is frequently employed in deep MVC since it supports the clustering objective. We present a semantics-guided contrastive multi-view clustering framework that takes advantage of the consistency and complementarity of views.

2.2 Contrastive learning.

Contrastive learning [6, 14] has proven to be quite effective in self-supervised learning in recent years. By creating positive and negative pairs, contrastive learning is able to obtain discriminative features. New perspectives on the difficulties of deep clustering are offered by the development of contrastive clustering [25]. In general, there are two types of multi-view contrastive clustering: instance-level contrastive learning [34, 42] and cluster-level contrastive learning [4]. [15, 41] make use of both. False negative pairs occur when setting negative pairs in the popular instance-level contrastive learning technique. In order to mitigate this issue, Trosten *et al.* [34] use negative pairs consisting of instances assigned to distinct clusters, whereas Yan *et al.* [42] add structure relationship to negative pairs. Semantics-guided instance-level contrastive learning and cluster-level contrastive learning are utilized in our framework. To reduce false negative pairs, instance pair weights derived from semantic features are introduced.

3 Method

In this section, we first explain the definitions used and the goal to be achieved in the framework. Next, we introduce the architecture of the framework. Finally, the total loss and entire optimization procedure are shown.

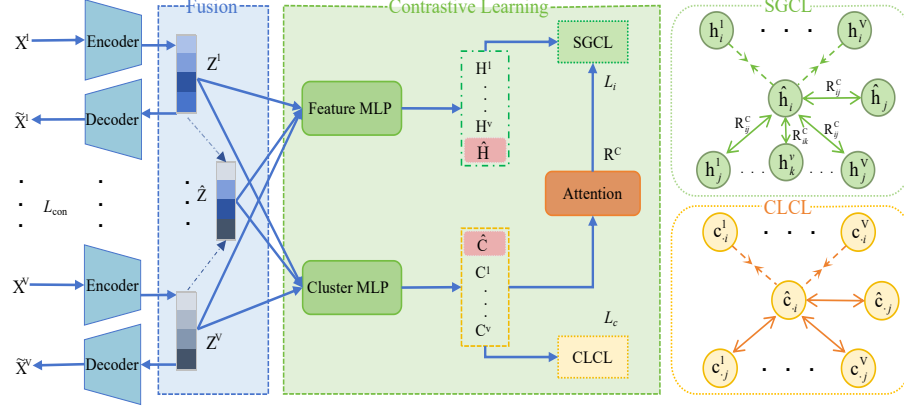


Fig. 1: The framework of DCMCS. The view-specific features Z^v , the fusion view features \hat{Z} , the instance-level features H^v, \hat{H} and the semantic features C^v, \hat{C} are learned from the raw features X^v . The reconstruction objective L_{con} is individually conducted on Z^v . In semantics-guided contrastive learning (SGCL) and cluster-level contrastive learning (CLCL) modules, two contrastive losses (i.e., L_i and L_c) are conducted on the instance-level features and cluster-level features, respectively. Moreover, R^C represents the weight matrix generated from semantic features to establish the relationship between negative pairs in L_i .

3.1 Proposed Statement

Given a multi-view dataset $\chi = \{X^v \in \mathbb{R}^{N \times D_v}\}_{v=1}^V$ with V views and N samples, $X^v = [x_1^v, x_2^v, \dots, x_N^v]$ denotes the instances of the v -th view. D_v denotes the feature dimension of the v -th view. Considering that there are K clusters in the dataset, the N samples are ultimately divided into K clusters according to their similarity.

3.2 View-specific feature fusion

The view-specific feature fusion module uses several view-specific autoencoders, as shown in Fig. 1, to extract the features of each view. In particular, we designate the encoder $f_{\theta_v}^v$ and the decoder $g_{\eta_v}^v$ for the v -th view, where θ_v and η_v are parameters of the encoder and decoder respectively. Encoder $f_{\theta_v}^v$ projects raw features into view-specific feature space by

$$z_i^v = f_{\theta_v}^v(x_i^v) \quad (1)$$

where $Z^v = [z_1^v, z_2^v, \dots, z_N^v]$, $Z^v \in \mathbb{R}^{N \times d}$. d is the dimension of the view-specific features. Inspired by [13], DCMCS employ decoder $g_{\eta_v}^v$ to reconstruct z_i^v to learn sufficient discriminative information avoiding the model collapsing.

$$\tilde{x}_i^v = g_{\eta_v}^v(z_i^v) = g_{\eta_v}^v(f_{\theta_v}^v(x_i^v)) \quad (2)$$

The reconstruction loss for all views is defined as:

$$L_{\text{con}} = \sum_{v=1}^V \left\| X^v - \tilde{X}^v \right\|_2^2 = \sum_{v=1}^V \sum_{i=1}^N \left\| x_i^v - g_{\eta^v}^v (f_{\theta^v}^v(x_i^v)) \right\|_2^2 \quad (3)$$

Weighted fusion is a simple and effective method for obtaining more discriminative fusion view features by leveraging the consistency and complementarity of multi-view data. Considering the importance of different views, we fuse the views using adaptive weighting to obtain the fusion view features $\hat{Z} \in \mathbb{R}^{N \times d}$, where $\hat{Z} = [\hat{z}_1, \hat{z}_2, \dots, \hat{z}_N]$. \hat{z}_i is defined as:

$$\hat{z}_i = \sum_{v=1}^V w_v z_i^v \quad (4)$$

where w_v is the v -th view's weight, $\sum_{v=1}^V w_v = 1$. The weights are obtained by loss function optimization, reflecting the importance of different views.

3.3 Cluster-level contrastive learning

Contrastive learning (CL) effectively captures high-level semantics while removing irrelevant information since it directly increases the feature similarity between semantically relevant instances. We apply cluster-level contrastive learning to improve cluster consistency across multiple views. A two-layer linear MLP with parameter W_C is utilized to map the view-specific features and fusion view features to K -dimension space. K is the number of clusters. A Softmax layer is attached to obtain the semantic features of each view $C^v = [c_1^v, c_2^v, \dots, c_N^v]$, $C^v \in \mathbb{R}^{N \times K}$ and the semantic features of the fusion view $\hat{C} = [\hat{c}_1, \hat{c}_2, \dots, \hat{c}_N]$, $\hat{C} \in \mathbb{R}^{N \times K}$. The semantic features are described by the probability that the instance belongs to each cluster. The instance's cluster label corresponds to the cluster with the highest probability. Cluster-level feature C_j^v is represented as the probability that each instance belongs to cluster j in the v -th view.

Since the instances in multiple views that correspond to a single sample share semantic information in common, the instances' cluster assignment probabilities across various views ought to be similar, and cluster-level features from the same cluster should be similar. Cluster-level contrastive learning increases the distance between cluster pairs corresponding to distinct clusters while decreasing the distance between cluster pairs corresponding to the same cluster. For each fusion view cluster-level feature \hat{c}_j , $\{\hat{c}_j, c_j^v\}_{v=1, \dots, V}$ are positive pairs and the rest cluster pairs of \hat{c}_j are negative pairs.

Cosine similarity is used to quantify the similarity between two clusters, which is explained as follows:

$$S(\hat{c}_j, c_j^v) = \frac{\langle \hat{c}_j, c_j^v \rangle}{\|\hat{c}_j\| \|c_j^v\|} \quad (5)$$

where $\langle \cdot, \cdot \rangle$ is the dot product operator. The cluster-level contrastive loss is defined as:

$$L_c = -\frac{1}{2K} \sum_{j=1}^K \sum_{v=1}^V \log \frac{e^{S(\hat{c}_j, c_j^v)/\tau_1}}{\sum_{k=1}^K e^{S(\hat{c}_j, c_k^v)/\tau_1} - e^{1/\tau_1}} - H(C) \quad (6)$$

where τ_1 denotes the temperature coefficient and $H(C)$ denotes the entropy of the clustering result. The presence of entropy prevents from falling into a trivial solution [16]. $H(C)$ is defined as follows:

$$H(C) = -\sum_{j=1}^K \left[\sum_{v=1}^V P(c_j^v) \log P(c_j^v) + P(\hat{c}_j) \log P(\hat{c}_j) \right] \quad (7)$$

where $P(c_j^v) = (\sum_{i=1}^N c_{ij}^v)/N$.

3.4 Semantics-guided instance-level contrastive learning

The quality of the positive and negative pairs construction are crucial factors in determining the performance of the contrastive MVC methods. A popular contrastive loss function in MVC is InfoNCE [6].

$$L_{\text{InfoNCE}} = -\log \left(\frac{\sum_{i=1}^N e^{S(z_i, z_i^+)/\tau}}{\sum_{j=1}^N e^{S(z_i, z_j)/\tau}} \right) \quad (8)$$

InfoNCE treats the instances in the different views corresponding to an individual sample as positive pairs and directly regards all other non-positive instances as negative pairs. This easily brings false negative pairs problems in that instances sharing the same cluster label are constructed as negative pairs, leading to cluster-unfriendly representation learning. To solve this problem, we propose a semantics-guided instance-level contrastive method by instance pair weights.

When calculating instance pair weights, rather than concentrating solely on the information in the specific views, we pay attention to the common information of the fusion view. The consistency and complementarity in the fusion view semantic features and specific view semantic features are taken into account. It can generate weights that are more precise and lessen the impact of view-private information in the fusion view. It produces superior clustering results, as demonstrated in Sec. 4.3.

Instance pair weights Semantic features of instances can be utilized to establish the instance relationship because instances in the same cluster have the same semantic information. Inspired by [42], the attention mechanism of transformer [36] is employed to evaluate the relationships between instances, as shown in Fig. 2. We first concatenate all specific view semantic features C^v and the semantic feature \hat{C} of the fusion view to get $C = [C^1, C^2, \dots, C^v, \hat{C}]$, $C \in \mathbb{R}^{n \times m}$,

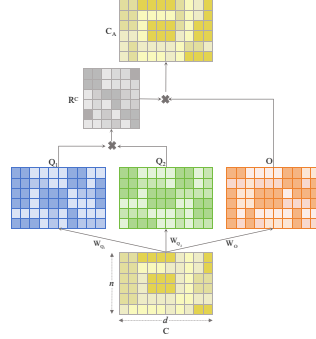


Fig. 2: Attention module. W_{Q_1} , W_{Q_2} , and W_O are utilized to achieve feature space transformation, and the weight matrix R^C is used to obtain instance pair weights.

where $m = (V + 1) \times K$. By including \hat{C} in the attention mechanism’s input, we can extract more important information from the fusion view and lessen the influence of view-private information. C is mapped to different feature spaces by W_{Q_1} , W_{Q_2} and W_O .

$$Q_1 = CW_{Q_1}; Q_2 = CW_{Q_2}; O = CW_O \quad (9)$$

where $Q_1 \in \mathbb{R}^{n \times m}$, $Q_2 \in \mathbb{R}^{n \times m}$, $Q_O \in \mathbb{R}^{n \times m}$. We use the matrix $W = \{W_{Q_1}, W_{Q_2}, W_O\}$ as the parameters.

The weight matrix R^C is defined as:

$$R^c = \text{Softmax}\left(\frac{Q_1 Q_2^T}{\sqrt{m}}\right) \quad (10)$$

The weight matrix R^C can represent the relationship between the instances, the higher the weight, the more similar the semantic features of the instance pairs and the higher the possibility of belonging to the same cluster. For negative instance pair (i, j) , the instance pair weight is defined as: $1 - R_{ij}^C$.

Instance-level contrastive learning under semantic guidance DCMCS apply instance-level contrastive learning to learn instance consistency across multiple views. Using a one-layer MLP, the instance-level features $H^v = [h_1^v, h_2^v, \dots, h_N^v]$, $H^v \in \mathbb{R}^{N \times d_h}$ of the specific view and the instance-level features $\hat{H} = [\hat{h}_1, \hat{h}_2, \dots, \hat{h}_N]$, $\hat{H} \in \mathbb{R}^{N \times d_h}$ of the fusion view are acquired. d_h is the dimension of the instance-level features. We denote the parameter of feature MLP as W_H . The instances that belong to an individual sample in the fusion view and specific views are considered as positive pairs, while all other non-positive instances are treated as negative pairs, with the fusion view serving as the anchor. The influence of false negative pairs in contrastive learning is weakened by instance pair weights.

Again, cosine similarity is utilized to measure the similarity between specific view instance-level features and fusion view instance-level features, defined as

follows:

$$S(\hat{\mathbf{h}}_i, \mathbf{h}_i^v) = \frac{\langle \hat{\mathbf{h}}_i, \mathbf{h}_i^v \rangle}{\|\hat{\mathbf{h}}_i\| \|\mathbf{h}_i^v\|} \quad (11)$$

The semantics-guided instance-level contrastive loss function is defined as:

$$L_i = -\frac{1}{2N} \sum_{i=1}^N \sum_{v=1}^V \log \frac{e^{S(\hat{\mathbf{h}}_i, \mathbf{h}_i^v)/\tau_2}}{\sum_{j=1}^N e^{(1-R_{ij}^C)S(\hat{\mathbf{h}}_i, \mathbf{h}_j^v)/\tau_2} - e^{1/\tau_2}} \quad (12)$$

where τ_2 denotes the temperature coefficient, and $1 - R_{ij}^C$ denotes the instance pair weights. R_{ij}^C is obtained from Eq. (10). A larger weight R_{ij}^C indicates a higher likelihood of the instance pair belonging to the same cluster, the instance pair weight $1 - R_{ij}^C$ is smaller. The instance pair weights can reduce the impact of false negative pairs and produce better cluster-friendly features.

3.5 Optimization

The final overall loss function is defined as follows:

$$L = L_{\text{con}} + \lambda_1 L_i + \lambda_2 L_c \quad (13)$$

Among them λ_1 and λ_2 are the balance parameters. According to parameter experiment in Sec. 4.4, we set λ_1 and λ_2 to 1. DCMCS obtain the cluster label y_i through the semantic features of the fusion view:

$$y_i = \arg \max(\hat{c}_i) \quad (14)$$

The final clustering results $Y = [y_1, y_2, \dots, y_N]$ for each sample are obtained. A summary of our optimization process is shown in Algorithm 1.

Algorithm 1 our optimization process

Input: Multi-view dataset $\{X^v\}_{v=1}^V$; Number of clusters K ;
Temperature parameters τ_1 and τ_2 ; Balance parameters
 λ_1 and λ_2 .

- 1: Initialize $\{\theta_v, \eta_v\}_{v=1}^V$ by minimizing Eq. (3);
- 2: Computing \hat{Z} via Eq. (4);
- 3: Optimize $W_H, W_C, \{\theta_v, \eta_v\}_{v=1}^V$ by minimizing Eq. (13)
- 4: Calculate semantic labels by Eq. (14)

Output: The label predictions $Y = [y_1, y_2, \dots, y_N]$.

4 Experiment

4.1 Experimental Setup

Datasets. Information about the five public datasets used for the experiments is given in Tab. 1. Synthetic3d [21] is a synthetic dataset containing 600 samples of 3 views. Hdigit [5] is a handwritten digit dataset obtained from MNIST

Table 1: The information of the datasets in our experiments

Datasets	Samples	Views	Classes
Synthetic3d	600	3	3
Hdigit	10000	2	10
Cifar10	50000	3	10
YouTube Face	101499	5	31
Caltech-5V	1400	5	7

Table 2: Whether fusion, instance-level contrastive learning, or cluster-level contrastive learning are used in the methods.

Method	Fusion	Instance-level	Cluster-level
EAMC (2020)	✓		
CONAN (2021)	✓	✓	
SiMVC (2021)	✓		
CoMVC (2021)	✓	✓	
MFLVC (2022)		✓	✓
CVCL (2023)			✓
AECoDDC (2023)	✓	✓	
GCFAgg (2023)	✓	✓	

Handwritten Digits and USPS Handwritten Digits. [Cifar10](http://www.cs.toronto.edu/kriz/cifar.html)¹ is a real RGB image dataset containing 10 clusters processed in the same way as in [42]. [YouTube-Face](https://www.cs.tau.ac.il/~wolf/ytfaces/)² is a massive face dataset with five views that are sourced from the YouTube video database. We divide Caltech-5V [11] into multiple datasets with different numbers of views. Caltech-5V contains views WM, CENTRIST, LBP, GIST, and HOG, Caltech-2V contains the first two views, Caltech-3V contains the first three views and Caltech-4V contains the first four views.

Comparison methods. EAMC [50] uses adversarial learning to align features of different views and employs attention layer to fuse views. CONAN [19] proposes a deep fusion module and introduces intermediate variable to align view-specific features. SiMVC [34] analyses the problems of alignment and uses weighted fusion view features to obtain clustering results. CoMVC [34] builds on SiMVC by adding instance-level contrastive learning and designing it as a selection. MFLVC [41] splits the learning of common information and view-specific features into two distinct levels of space, performing contrastive learning at the high-level features. The cluster allocation results are further optimized for cluster-level contrastive learning using CVCL [4]. AECoDDC is one of the approaches under the generalized framework proposed in [35]. It

¹ <http://www.cs.toronto.edu/kriz/cifar.html>

² <https://www.cs.tau.ac.il/~wolf/ytfaces/>

aligns view features with contrastive learning. GCFAgg [42] proposes a structure-guided instance-level contrastive loss to achieve consistency goal. Tab. 2 displays whether these methods make use of fusion, instance-level contrastive learning, or cluster-level contrastive learning.

Evaluation metrics. The clustering effectiveness is evaluated by three metrics: clustering accuracy (ACC), normalized mutual information (NMI), and purity (PUR).

Implementation. The experimental framework is implemented on the Pytorch platform and executed on a 24GB NVIDIA Geforce RTX 3090 Linux server. The encoder and decoder are implemented using fully connected layers with encoder dimensions of input-500-500-2000-512. The decoder is symmetric with encoder. Adam optimizer is adopted with a learning rate of 0.0003 and a batch size of 256. The experiments use the reconstruction loss to pre-train for 200 epochs, followed by 100 or 150 epochs using the overall loss function. The code will be released.

4.2 Performance Analysis

The experimental results on four datasets are shown in Tab. 3, from which we could have the following findings: (1) Our DCMCS achieves the best results on all metrics. DCMCS performs 2% better on NMI than the best comparable method, AECoDDC, on the Synthetic3d dataset. This is because **we employ semantics-guided instance-level contrastive learning, which weakens the effect of false negative pairs.** (2) Tab. 2 presents the usage of instance-level contrastive learning and cluster-level contrastive learning in the comparison methods. As we account for both of them and introduce instance pair weights, our DCMCS performs better. **DCMCS combines instance-level contrastive learning with clustering goal, obtaining instance relationships through semantic features rather than view-specific features like GCFAgg.** (3) The comparison methods with and without fusion are also depicted in the Tab. 2.

Table 3: Results of all methods on four datasets. Bold denotes the best results and underline denotes the second-best.

Datasets	Synthetic3d			Hdigit			Cifar10			YouTubuFace		
Metrics	ACC	NMI	PUR	ACC	NMI	PUR	ACC	NMI	PUR	ACC	NMI	PUR
EAMC (2020)	0.9333	0.7688	0.9333	0.4878	0.5151	0.4939	0.4533	0.3824	0.4574	0.1366	0.0369	0.2662
CONAN (2021)	0.9650	0.8540	0.9650	0.9562	0.9193	0.9562	0.9255	0.8641	0.9255	0.1179	0.1178	0.1499
SIMVC (2021)	0.9366	0.7747	0.9366	0.7854	0.6705	0.7854	0.8359	0.7324	0.8359	0.0765	0.0481	0.2662
CoMVC (2021)	0.9530	0.8184	0.9520	0.9032	0.8713	0.9032	0.9275	0.8925	0.9275	0.1010	0.0851	0.2674
MFLVC (2022)	0.9650	0.8537	0.9650	0.9442	0.8750	0.9440	0.9918	0.9774	0.9918	0.2770	0.2952	0.3297
CVCL (2023)	0.6367	0.4188	0.6500	0.3216	0.2407	0.3227	0.9910	0.9755	0.9910	0.3116	<u>0.3431</u>	0.3840
AECoDDC (2023)	<u>0.9750</u>	<u>0.8927</u>	<u>0.9750</u>	<u>0.9930</u>	<u>0.9796</u>	<u>0.9930</u>	0.8594	0.7590	0.8594	0.2703	0.2789	0.3578
GCFAgg (2023)	0.9700	0.8713	0.9700	0.9744	0.9305	0.9744	<u>0.9923</u>	<u>0.9781</u>	<u>0.9923</u>	<u>0.3262</u>	0.3289	<u>0.4007</u>
DCMCS(ours)	0.9817	0.9127	0.9817	0.9940	0.9811	0.9940	0.9929	0.9805	0.9929	0.3355	0.3508	0.4302

Table 4: Results of all methods on Caltech with different views. "-XV" indicates that there are X views available.

Datasets	Caltech-2V			Caltech-3V			Caltech-4V			Caltech-5V		
Metrics	ACC	NMI	PUR	ACC	NMI	PUR	ACC	NMI	PUR	ACC	NMI	PUR
EAMC (2020)	0.4993	0.4449	0.5207	0.5014	0.3617	0.5029	0.4786	0.3709	0.4786	0.3936	0.3540	0.4000
CONAN (2021)	0.5750	0.4516	0.5757	0.5914	0.4981	0.5914	0.5571	0.5061	0.5735	0.7207	0.6418	0.7221
SiMVC (2021)	0.5083	0.4715	0.5573	0.5692	0.4953	0.5912	0.6193	0.5362	0.6303	0.7193	0.6771	0.7292
CoMVC (2021)	0.4663	0.4262	0.5272	0.5413	0.5043	0.5842	0.5683	0.5692	0.6463	0.7003	0.6871	0.7462
MFLVC (2022)	0.6060	0.5280	0.6160	0.6312	0.5663	0.6392	0.7332	0.6523	0.7342	0.8042	0.7032	0.8043
CVCL (2023)	0.6479	0.5503	0.6479	0.6664	0.5493	0.6664	0.6643	0.5934	0.6864	0.7457	0.6549	0.5903
AECoDDC (2023)	0.4579	0.3410	0.4607	0.5857	0.4549	0.6057	0.4893	0.3923	0.5271	0.6564	0.5898	0.6786
GCFAgg (2023)	0.6643	0.5008	0.6643	0.6400	0.5345	0.6529	0.7343	0.6610	0.7343	0.8336	0.7331	0.8336
DCMCS(ours)	0.6664	0.5709	0.6664	0.7543	0.6582	0.7600	0.8464	0.7291	0.8464	0.8907	0.8172	0.8907

Each view feature includes common and meaningless view-private information [41]. The importance of each view is taken into consideration by the fusion view. However, the issue of view fusion-related representational deterioration can also affect the clustering results [40]. **We use weighted fusion to alleviate the representation degradation problem and focus on the common information of the fused views to further alleviate the interference of view-private information.**

We further analyze DCMCS’s performance on datasets with varying numbers of views using the Caltech dataset. The results in Tab. 4 indicate that (1) The efficiency of our approach gets better as the number of views rises. It proves that DCMCS is robust on datasets with different number of views. (2) Compared to the best method, GCFAgg, DCMCS increases ACC metric on the Caltech-4V dataset by around 13%. The quality of the Caltech dataset varies depending on the view, as seen in [40]. **The semantic features we adopted are more useful when there are significant variations across views.** (3) Compared to the methods MFLVC and CVCL which do not use fusion, our method improves ACC about 16% and 11% on Caltech-3V respectively, proving considering the importance of the different views is important.

In Fig. 3, the visualization of GCFAgg Fig. 3a-Fig. 3c and our DCMCS Fig. 3d-Fig. 3f are achieved through the application of t-SNE on the two views of Hdigit and the fusion view. Our approach, in contrast to GCFAgg, enhances the clustering effect of views, resulting in a more compact intra-cluster structure and farther-separating inter-clusters. This is due to the fact that we introduce instance pair weights using semantic features and take into account cluster-level contrastive learning.

4.3 Ablation Studies

Loss components. We use two datasets with distinct properties for the loss function ablation studies. Caltech-5V is a tiny dataset with varying view quality; Hdigit is large, and the two views’ clustering accuracy is very little different, at 0.9420 and 0.9637. Tab. 5 displays the optimal results for both datasets that incorporate all loss functions. In case (a), we apply k-means [1] on the \hat{Z} to achieve

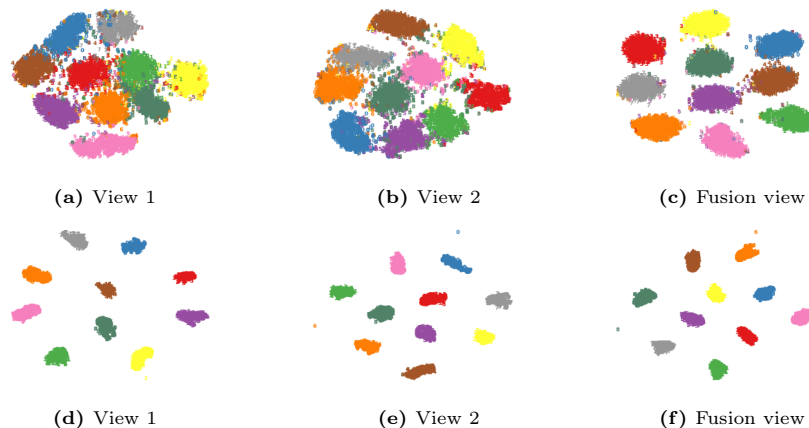


Fig. 3: Visualization of GCFagg (a-c) and DCMCS (d-f) on Hdigit’s two views and fusion view

Table 5: Ablation studies on loss components

	Components			Caltech-5V		Hdigit	
	L_{con}	L_i	L_c	ACC	NMI	ACC	NMI
(a)	✓			0.8850	0.7957	0.9387	0.8636
(b)	✓	✓		0.4357	0.4387	0.9525	0.9091
(c)	✓		✓	0.7157	0.6566	0.9919	0.9753
(d)	✓	✓	✓	0.8907	0.8172	0.9940	0.9811
(e)			✓	0.6657	0.5661	0.9933	0.9791

clustering results. The findings show that improved features can be learned in the reconstruction. We use k-means on the \hat{H} in (b) to obtain clustering results. In comparison to (a), it improves on Hdigit but drastically degrades on Caltech-5V. When there is an adequate number of instances, instance-level contrastive learning is more helpful. In case (c), the Caltech-5V dataset effect is enhanced by about 39% on ACC, which is consistent with the effect of [4]. In addition, we attempt to remove the pre-training in (e), and the reduction is roughly 25% on Caltech-5V and only 0.07% on Hdigit. It suggests that in order to keep the model from crashing, pre-training is crucial on tiny datasets with varying view quality.

Effectiveness of R^C . The experimental results are shown in Tab. 6 and Tab. 7. The effect is better with R^C than without it. The effect is improved by roughly 9.5% on the ACC metric on the YouTubeFace dataset and somewhat on the Synthetic3d, Hdigit, and Cifar10 datasets. On datasets with large view quality disparities, Caltech-5V, the effect is significantly improved, with an average im-

Table 6: Ablation studies with or without R^C on different datasets

Datasets	Synthetic3d			Hdigit			Cifar10			YouTubuFace		
Metrics	ACC	NMI	PUR	ACC	NMI	PUR	ACC	NMI	PUR	ACC	NMI	PUR
w R^C	0.9817	0.9127	0.9817	0.9940	0.9811	0.9940	0.9929	0.9805	0.9929	0.3355	0.3508	0.4302
w/o R^C	0.9800	0.9066	0.9800	0.9923	0.9766	0.9923	0.9916	0.9784	0.9916	0.3037	0.3306	0.4059

Table 7: Ablation studies with or without R^C on Caltech

Datasets	Caltech-2V			Caltech-3V			Caltech-4V			Caltech-5V		
Metrics	ACC	NMI	PUR	ACC	NMI	PUR	ACC	NMI	PUR	ACC	NMI	PUR
w R^C	0.6664	0.5709	0.6664	0.7543	0.6582	0.7600	0.8464	0.7291	0.8464	0.8907	0.8172	0.8907
w/o R^C	0.5200	0.4262	0.5264	0.7064	0.6115	0.7350	0.7400	0.6762	0.7557	0.8314	0.7412	0.8314

provement of nearly 11% on ACC. The influence of false negative pairs and the conflict between instance-level contrastive learning and the clustering target can be lessened when R^C is present. As a result, it is more suited for the clustering task, especially for views with significant quality differences.

Table 8: Ablation study on using R^C or R^H , and whether \hat{C} is added to R^C and \hat{H} is added to R^H .

Datasets	Synthetic3d			Hdigit			Cifar10			YouTubuFace		
Metrics	ACC	NMI	PUR	ACC	NMI	PUR	ACC	NMI	PUR	ACC	NMI	PUR
R^C w \hat{C}	0.9817	0.9127	0.9817	0.9940	0.9811	0.9940	0.9929	0.9805	0.9929	0.3355	0.3508	0.4302
R^C w/o \hat{C}	0.9783	0.9028	0.9783	0.9933	0.9797	0.9933	0.9918	0.9776	0.9918	0.3299	0.3495	0.4230
R^H w \hat{H}	0.9800	0.9078	0.9800	0.9937	0.9805	0.9937	0.9891	0.9718	0.9891	0.3024	0.3341	0.3846
R^H w/o \hat{H}	0.9750	0.8899	0.9750	0.9925	0.9768	0.9925	0.9860	0.9644	0.9860	0.2931	0.3316	0.3770

Comparison between R^C and R^H We analyze whether to employ semantic features to create the weight matrix R^C rather than instance-level features to produce R^H , as well as whether to use the fusion view when generating R^C and R^H . Tab. 8 shows that the results obtained with R^C are better than those obtained with R^H , with an improvement of 9.87% on the YouTubuFace dataset on ACC. Because semantic features allow for a more accurate measurement of the relationship between instances. Furthermore, we note that joining \hat{C} in acquiring R^C and adding \hat{H} at the time of obtaining R^H both produce better results than not adding. This is because we focus on the common information of \hat{C} , \hat{H} and alleviate the interference caused by view-private information of the fusion view.

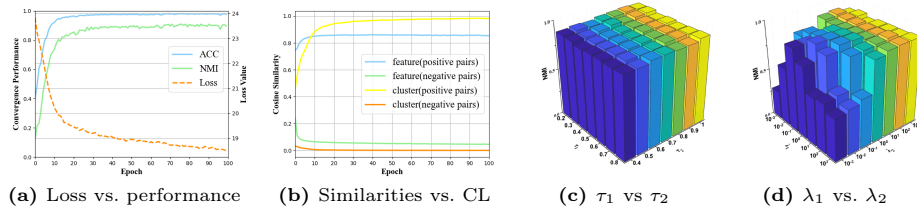


Fig. 4: (a) Convergence analysis. (b) The similarities of feature pairs and cluster pairs in contrastive learning(CL). (c) and (d) Parameters sensitivity analysis.

4.4 Parameter Analysis.

Convergence analysis. Fig. 4a illustrates how loss decreases as ACC and NMI increase until stability. DCMCS enjoys great convergence property. Fig. 4b displays instances and clusters’ positive and negative similarities. Instance-level features and cluster-level features show an increase in positive pairwise similarity and a drop in negative pairwise similarity after training. It matches our objective of clustering.

Parameter sensitivity analysis. Through Fig. 4c, we observe that the choice of temperature coefficients is insensitive for the semantics-guided instance-level contrastive loss and cluster-level contrastive loss. We set $\tau_1 = 1.0$ and $\tau_2 = 0.5$ empirically. The overall loss function’s hyper-parameters are denoted as λ_1 and λ_2 . We can see from Fig. 4d that the model is insensitive when the λ_1 is at $10^{-1} \sim 10^3$ and λ_2 is at $10^0 \sim 10^3$. We set $\lambda_1 = 1$ and $\lambda_2 = 1$ for convenience.

5 Conclusion

In this paper, we propose a semantics-guided contrastive multi-view clustering framework. Weighted fusion is used to fuse the features of views based on how important each view is. To lessen false negative pairs, instance pair weights are obtained from the semantic features of the fusion view and specific views through the attention mechanism. Furthermore, we minimize the influence of view-private information in the fusion view by concentrating on its common information. Experimental results on several public datasets demonstrate that DCMCS outperforms the state-of-the-art methods. Our framework’s drawback is that it can be simple to assign the incorrect cluster when there are super-classes in the dataset, which leads to the instance being split up into a few clusters. We will address this issue in our future work.

References

1. Bauckhage, C.: K-means clustering is matrix factorization. arXiv preprint arXiv:1512.07548 (2015) 11

2. Chen, C., Li, X., Ng, M.K., Yuan, X.: Total variation based tensor decomposition for multi-dimensional data with time dimension. *Numerical Linear Algebra with Applications* **22**(6), 999–1019 (2015) [1](#)
3. Chen, J., Mao, H., Peng, D., Zhang, C., Peng, X.: Multiview clustering by consensus spectral rotation fusion. *IEEE Transactions on Image Processing* (2023) [1](#), [3](#)
4. Chen, J., Mao, H., Woo, W.L., Peng, X.: Deep multiview clustering by contrasting cluster assignments. *arXiv preprint arXiv:2304.10769* (2023) [3](#), [9](#), [12](#)
5. Chen, M.S., Lin, J.Q., Li, X.L., Liu, B.Y., Wang, C.D., Huang, D., Lai, J.H.: Representation learning in multi-view clustering: A literature review. *Data Science and Engineering* **7**(3), 225–241 (2022) [8](#)
6. Chen, T., Kornblith, S., Norouzi, M., Hinton, G.: A simple framework for contrastive learning of visual representations. In: *International conference on machine learning*. pp. 1597–1607. PMLR (2020) [2](#), [3](#), [6](#)
7. Chen, W., Wang, H., Liang, C.: Deep multi-view contrastive learning for cancer subtype identification. *Briefings in Bioinformatics* **24**(5), bbad282 (2023) [1](#)
8. Chen, Z., Li, Y., Lou, K., Zhao, L.: Incomplete multi-view clustering with complete view guidance. *IEEE Signal Processing Letters* (2023) [3](#)
9. Cui, C., Ren, Y., Pu, J., Pu, X., He, L.: Deep multi-view subspace clustering with anchor graph. *arXiv preprint arXiv:2305.06939* (2023) [3](#)
10. Fang, U., Li, M., Li, J., Gao, L., Jia, T., Zhang, Y.: A comprehensive survey on multi-view clustering. *IEEE Transactions on Knowledge and Data Engineering* (2023) [1](#)
11. Fei-Fei, L., Fergus, R., Perona, P.: Learning generative visual models from few training examples: An incremental bayesian approach tested on 101 object categories. In: *2004 conference on computer vision and pattern recognition workshop*. pp. 178–178. IEEE (2004) [9](#)
12. Guo, J., Ye, J.: Anchors bring ease: An embarrassingly simple approach to partial multi-view clustering. In: *Proceedings of the AAAI conference on artificial intelligence*. vol. 33, pp. 118–125 (2019) [1](#)
13. Guo, X., Gao, L., Liu, X., Yin, J.: Improved deep embedded clustering with local structure preservation. In: *Ijcai*. vol. 17, pp. 1753–1759 (2017) [4](#)
14. He, K., Fan, H., Wu, Y., Xie, S., Girshick, R.: Momentum contrast for unsupervised visual representation learning. In: *Proceedings of the IEEE/CVF conference on computer vision and pattern recognition*. pp. 9729–9738 (2020) [3](#)
15. Hu, S., Zou, G., Zhang, C., Lou, Z., Geng, R., Ye, Y.: Joint contrastive triple-learning for deep multi-view clustering. *Information Processing & Management* **60**(3), 103284 (2023) [2](#), [3](#)
16. Hu, W., Miyato, T., Tokui, S., Matsumoto, E., Sugiyama, M.: Learning discrete representations via information maximizing self-augmented training. In: *International conference on machine learning*. pp. 1558–1567. PMLR (2017) [6](#)
17. Jin, Y., Li, C., Li, Y., Peng, P., Giannopoulos, G.A.: Model latent views with multi-center metric learning for vehicle re-identification. *IEEE Transactions on Intelligent Transportation Systems* **22**(3), 1919–1931 (2021) [1](#)
18. Kang, Z., Shi, G., Huang, S., Chen, W., Pu, X., Zhou, J.T., Xu, Z.: Multi-graph fusion for multi-view spectral clustering. *Knowledge-Based Systems* **189**, 105102 (2020) [1](#)
19. Ke, G., Hong, Z., Zeng, Z., Liu, Z., Sun, Y., Xie, Y.: Conan: contrastive fusion networks for multi-view clustering. In: *2021 IEEE International Conference on Big Data (Big Data)*. pp. 653–660. IEEE (2021) [2](#), [9](#)

20. Ke, G., Zhu, Y., Yu, Y.: Mori-ran: Multi-view robust representation learning via hybrid contrastive fusion. In: 2022 IEEE International Conference on Data Mining Workshops (ICDMW). pp. 467–474. IEEE (2022) [2](#)
21. Kumar, A., Rai, P., Daume, H.: Co-regularized multi-view spectral clustering. *Advances in neural information processing systems* **24** (2011) [8](#)
22. Lan, S., Zheng, Q., Yu, Y.: Double-level view-correlation multi-view subspace clustering. *Knowledge-Based Systems* **284**, 111271 (2024) [1](#), [3](#)
23. Li, L., He, H.: Bipartite graph based multi-view clustering. *IEEE transactions on knowledge and data engineering* **34**(7), 3111–3125 (2020) [3](#)
24. Li, W., Wang, S., Guo, X., Zhu, E.: Deep graph clustering with multi-level subspace fusion. *Pattern Recognition* **134**, 109077 (2023) [3](#)
25. Li, Y., Hu, P., Liu, Z., Peng, D., Zhou, J.T., Peng, X.: Contrastive clustering. In: *Proceedings of the AAAI conference on artificial intelligence*. vol. 35, pp. 8547–8555 (2021) [3](#)
26. Li, Z., Wang, Q., Tao, Z., Gao, Q., Yang, Z., et al.: Deep adversarial multi-view clustering network. In: *IJCAI*. vol. 2, p. 4 (2019) [3](#)
27. Liang, W., Zhou, S., Xiong, J., Liu, X., Wang, S., Zhu, E., Cai, Z., Xu, X.: Multi-view spectral clustering with high-order optimal neighborhood laplacian matrix. *IEEE Transactions on Knowledge and Data Engineering* **34**(7), 3418–3430 (2020) [1](#), [3](#)
28. Liu, D., Peng, S.J., Liu, X., Zhu, L., Cui, Z., Li, T.: Inconsistency distillation for consistency: Enhancing multi-view clustering via mutual contrastive teacher-student learning. In: 2022 IEEE International Conference on Data Mining (ICDM). pp. 251–258. IEEE (2022) [3](#)
29. Liu, J., Wang, C., Gao, J., Han, J.: Multi-view clustering via joint nonnegative matrix factorization. In: *Proceedings of the 2013 SIAM international conference on data mining*. pp. 252–260. SIAM (2013) [1](#)
30. Long, Z., Zhu, C., Chen, J., Li, Z., Ren, Y., Liu, Y.: Multi-view mera subspace clustering. *arXiv preprint arXiv:2305.09095* (2023) [3](#)
31. Peng, X., Feng, J., Zhou, J.T., Lei, Y., Yan, S.: Deep subspace clustering. *IEEE transactions on neural networks and learning systems* **31**(12), 5509–5521 (2020) [1](#), [3](#)
32. Ramon Soria, P., Sukkar, F., Martens, W., Arrue, B.C., Fitch, R.: Multi-view probabilistic segmentation of pome fruit with a low-cost rgb-d camera. In: *ROBOT 2017: Third Iberian Robotics Conference: Volume 2*. pp. 320–331. Springer (2018) [1](#)
33. Tan, Y., Liu, Y., Huang, S., Feng, W., Lv, J.: Sample-level multi-view graph clustering. In: *Proceedings of the IEEE/CVF Conference on Computer Vision and Pattern Recognition*. pp. 23966–23975 (2023) [1](#), [3](#)
34. Trosten, D.J., Lokse, S., Jenssen, R., Kampffmeyer, M.: Reconsidering representation alignment for multi-view clustering. In: *Proceedings of the IEEE/CVF conference on computer vision and pattern recognition*. pp. 1255–1265 (2021) [1](#), [3](#), [9](#)
35. Trosten, D.J., Løkse, S., Jenssen, R., Kampffmeyer, M.C.: On the effects of self-supervision and contrastive alignment in deep multi-view clustering. In: *Proceedings of the IEEE/CVF Conference on Computer Vision and Pattern Recognition*. pp. 23976–23985 (2023) [9](#)
36. Vaswani, A., Shazeer, N., Parmar, N., Uszkoreit, J., Jones, L., Gomez, A.N., Kaiser, Ł., Polosukhin, I.: Attention is all you need. *Advances in neural information processing systems* **30** (2017) [6](#)

37. Wang, Y., Chang, D., Fu, Z., Zhao, Y.: Consistent multiple graph embedding for multi-view clustering. *IEEE transactions on multimedia* (2021) [1](#)
38. Wen, J., Liu, C., Xu, G., Wu, Z., Huang, C., Fei, L., Xu, Y.: Highly confident local structure based consensus graph learning for incomplete multi-view clustering. In: *Proceedings of the IEEE/CVF Conference on Computer Vision and Pattern Recognition*. pp. 15712–15721 (2023) [1](#), [3](#)
39. Xie, D., Gao, Q., Wang, Q., Zhang, X., Gao, X.: Adaptive latent similarity learning for multi-view clustering. *Neural Networks* **121**, 409–418 (2020) [1](#)
40. Xu, J., Chen, S., Ren, Y., Shi, X., Shen, H., Niu, G., Zhu, X.: Self-weighted contrastive learning among multiple views for mitigating representation degeneration. *Advances in Neural Information Processing Systems* **36** (2024) [2](#), [11](#)
41. Xu, J., Tang, H., Ren, Y., Peng, L., Zhu, X., He, L.: Multi-level feature learning for contrastive multi-view clustering. In: *Proceedings of the IEEE/CVF Conference on Computer Vision and Pattern Recognition*. pp. 16051–16060 (2022) [2](#), [3](#), [9](#), [11](#)
42. Yan, W., Zhang, Y., Lv, C., Tang, C., Yue, G., Liao, L., Lin, W.: Gcfagg: Global and cross-view feature aggregation for multi-view clustering. In: *Proceedings of the IEEE/CVF Conference on Computer Vision and Pattern Recognition*. pp. 19863–19872 (2023) [3](#), [6](#), [9](#), [10](#)
43. Yang, W., Wang, Y., Tang, C., Tong, H., Wei, A., Wu, X.: One step multi-view spectral clustering via joint adaptive graph learning and matrix factorization. *Neurocomputing* **524**, 95–105 (2023) [3](#)
44. Yang, X., Xu, W., Leng, D., Wen, Y., Wu, L., Li, R., Huang, J., Bo, X., He, S.: Exploring novel disease-disease associations based on multi-view fusion network. *Computational and Structural Biotechnology Journal* **21**, 1807–1819 (2023) [1](#)
45. Yang, X., Deng, C., Dang, Z., Tao, D.: Deep multiview collaborative clustering. *IEEE Transactions on Neural Networks and Learning Systems* (2021) [1](#), [3](#)
46. Yin, J., Sun, S.: Incomplete multi-view clustering with cosine similarity. *Pattern Recognition* **123**, 108371 (2022) [1](#)
47. Yu, H., Zhang, T., Chen, J., Guo, C., Lian, Y.: Web items recommendation based on multi-view clustering. In: *2018 IEEE 42nd annual computer software and applications conference (COMPSAC)*. vol. 1, pp. 420–425. IEEE (2018) [1](#)
48. Zhang, L., Lin, L., Li, J.: Multi-view clustering by cps-merge analysis with application to multimodal single-cell data. *PLOS Computational Biology* **19**(4), e1011044 (2023) [1](#)
49. Zhong, G., Pun, C.M.: Self-taught multi-view spectral clustering. *Pattern Recognition* **138**, 109349 (2023) [3](#)
50. Zhou, R., Shen, Y.D.: End-to-end adversarial-attention network for multi-modal clustering. In: *Proceedings of the IEEE/CVF conference on computer vision and pattern recognition*. pp. 14619–14628 (2020) [3](#), [9](#)
51. Zhou, Y., Zheng, Q., Wang, Y., Yan, W., Shi, P., Zhu, J.: Mcoco: Multi-level consistency collaborative multi-view clustering. *Expert Systems with Applications* **238**, 121976 (2024) [3](#)
52. Zong, L., Zhang, X., Liu, X.: Multi-view clustering on unmapped data via constrained non-negative matrix factorization. *Neural Networks* **108**, 155–171 (2018) [1](#)